

**Effect of Water Content on the Corrosion Behavior of Carbon Steel in Supercritical CO<sub>2</sub> Phase with Impurities**

Yoon-Seok Choi  
Institute for Corrosion and Multiphase Technology,  
Department of Chemical and Biomolecular Engineering, Ohio University  
342 West State Street  
Athens, OH 45701  
USA

Srdjan Nešić  
Institute for Corrosion and Multiphase Technology,  
Department of Chemical and Biomolecular Engineering, Ohio University  
342 West State Street  
Athens, OH 45701  
USA

**ABSTRACT**

Sufficient drying (water removal) of carbon dioxide (CO<sub>2</sub>) in transport pipelines is required to prevent breaking-out of free water and consequent excessive corrosion rates. The drying requirement for CO<sub>2</sub> pipelines, used for enhanced oil recovery (EOR) in the United States, is a maximum of 650 ppm (mole) of water. However, there is a possibility of increased corrosion rates in supercritical CO<sub>2</sub> phase with water vapor (below its solubility level) in the presence of oxygen (O<sub>2</sub>) and sulfur dioxide (SO<sub>2</sub>). Thus, the objective of the present study is to evaluate the corrosion properties of carbon steel in supercritical CO<sub>2</sub>/O<sub>2</sub>/SO<sub>2</sub> mixtures with different amounts of water (under-saturated) related to the transmission of CO<sub>2</sub> to sequestration sites. The corrosion property of carbon steel was evaluated by using an autoclave operating at different pressures (maximum 2000 psi), temperatures (maximum 50°C), and concentrations of O<sub>2</sub> and SO<sub>2</sub> impurities as well as water content. The corrosion rate of samples was determined by weight loss measurements. The surface morphology and the composition of the corrosion product layers were analyzed using surface analytical techniques (scanning electron microscopy (SEM), energy dispersive spectroscopy (EDS) and X-ray diffraction (XRD)).

Key words: Supercritical CO<sub>2</sub>, CO<sub>2</sub> corrosion, H<sub>2</sub>O, O<sub>2</sub>, SO<sub>2</sub>, carbon steel, carbon capture and storage

**INTRODUCTION**

It is well known that dry CO<sub>2</sub> does not corrode carbon steels generally used for pipelines, as long as the relative humidity is less than 60%.<sup>1</sup> Thus, sufficient drying (water removal) upstream of the pipeline is standard practice in order to prevent excessive corrosion rates.<sup>2,3</sup> The drying requirement for CO<sub>2</sub>

pipelines, for example, used for enhanced oil recovery (EOR) in the United States, is to a maximum of 650 ppm (mole) water.<sup>4</sup>

Although water can be near completely removed or its concentration fixed below the required level, real CO<sub>2</sub> streams – those from CO<sub>2</sub> capture plants likely to contain impurities as opposed to pure CO<sub>2</sub> streams – will likely be 95 mole % CO<sub>2</sub> and will also contain impurities generated in the individual power plant and carbon capture-related facilities.<sup>5</sup>

According to our previous results, the addition of SO<sub>2</sub> in the gas phase dramatically increased the corrosion rate of carbon steel in a water-saturated CO<sub>2</sub> phase from 0.38 to 5.6 mm/y. This further increased to more than 7 mm/y with addition of both O<sub>2</sub> and SO<sub>2</sub>.<sup>6</sup> These results indicated that corrosion can take place in the water-saturated supercritical CO<sub>2</sub> phase in the presence of impurities. Water-saturated supercritical CO<sub>2</sub> is both highly diffusive, due to its low viscosity, and highly reactive owing to the potentially enhanced acidic nature of water dissolved in the dense CO<sub>2</sub> phase containing impurities. Changes in speciation are likely to occur, such as formation of sulfurous acid:



In terms of corrosion, SO<sub>2</sub> and water could then act as synergists with markedly enhanced corrosion rates.

Recent research<sup>7</sup> showed that water solvated in liquid and supercritical CO<sub>2</sub> is quite reactive towards the steel surface under conditions that approximate those anticipated for CO<sub>2</sub> transport. No corrosion was observed on carbon steel in liquid CO<sub>2</sub> with 610 ppmw water at 62 bar and 22°C for 42 days. With 998 ppmw water, however, corrosion product formed on the steel over 21 days at the same working pressure and temperature. Water solubility in liquid CO<sub>2</sub> at 63 bar and 22°C is approximately 1100 ppmw, this implies that corrosion occurs in the liquid CO<sub>2</sub> phase when under-saturated with respect to water. In addition, it suggests that there is a threshold water content for onset of corrosion. Other research<sup>8</sup> claimed that the corrosion rate of carbon steel in the presence of a small quantity of water (1000 ppm) in supercritical CO<sub>2</sub> was 1 mm/y at 79 bar and 31°C. Furthermore, even with water content lower than Kinder Morgan specification (650 ppm), there is a possibility for corrosion at certain conditions.<sup>9</sup>

Since all of these researches did not consider the effect of impurities such as O<sub>2</sub> and SO<sub>2</sub>, it can be hypothesized that if there is the possibility of corrosion with very small amounts of water in supercritical CO<sub>2</sub>, then it would be accelerated by the presence of O<sub>2</sub> and SO<sub>2</sub>. Thus, the objective of the present study was to test this hypothesis and to evaluate the corrosion properties of carbon steel in supercritical CO<sub>2</sub>/O<sub>2</sub>/SO<sub>2</sub> mixtures with different amounts of water (under-saturated) related to the transmission of CO<sub>2</sub> to sequestration sites.

## EXPERIMENTAL PROCEDURE

The test specimens were machined from carbon steel (API<sup>(1)</sup> 5L X65) with a size of 25 X 15 X 4 mm. A 1 mm diameter hole at one end serves to hang the samples from a sample stand with a non-metallic wire inside the autoclave. The composition of this steel is given in Table 1.

The specimens were ground with 600 grit silicon carbide paper, cleaned with isopropyl alcohol in an ultrasonic bath, dried, and weighed using a balance with a precision of 0.1 mg. The electrolyte used in this work was deionized (DI) water.

---

<sup>(1)</sup> American Petroleum Institute (API), 1220 L St. NW, Washington, DC 20005.

**TABLE 1**  
**ELEMENT ANALYSIS FOR THE CARBON STEEL (API<sup>(2)</sup> 5L X65) USED IN THE TESTS (WT %),**  
**BALANCE Fe**

	C	Mn	Si	P	S	Cr	Cu	Ni	Mo	Al	V
X65	0.065	1.54	0.25	0.013	0.001	0.05	0.04	0.04	0.007	0.041	-

The weight loss experiments were performed in a 2000 psi static autoclave with 1000 ml volume. Technical grade (ultra high purity) oxygen (O<sub>2</sub>) and sulfur dioxide (SO<sub>2</sub>) cylinders served as the O<sub>2</sub> and SO<sub>2</sub> sources which were directly added to the autoclave by adjustment of the partial pressures of each gas. High pressure CO<sub>2</sub> was added to the autoclave with gas booster pump to the desired working pressure. Further details of the experimental setup can be found in our previous paper.<sup>6</sup>

The corrosion rates were determined from the weight-loss method at the end of 24-hour or 120-hour exposures. In each test, two specimens were simultaneously exposed to the corrosive environment in order to obtain an averaged corrosion rate. The specimens were removed and cleaned for 5 min in Clarke solution (20 g antimony trioxide + 50 g stannous chloride and hydrochloric acid to make 1000 ml).<sup>10</sup> The specimens were then rinsed in distilled water, dried and weighed to 0.1 mg. The average corrosion rate during the test period can be calculated by the following equation:<sup>11</sup>

$$\text{Corrosion rate (mm/y)} = \frac{8.76 \times 10^4 (\text{mm} \cdot \text{hour/cm} \cdot \text{year}) \times \text{weight loss (g)}}{\text{area (cm}^2\text{)} \times \text{density (g/cm}^3\text{)} \times \text{time (hour)}} \quad (2)$$

The morphology and compositions of corrosion products were analyzed by scanning electron microscopy (SEM), energy dispersive X-ray spectroscopy (EDS) and X-ray diffraction (XRD).

### Effect of Water Content on the Corrosion of Carbon Steel in the Supercritical CO<sub>2</sub>/O<sub>2</sub> Phase

Table 2 shows the test matrix for corrosion in supercritical CO<sub>2</sub>/O<sub>2</sub> phases with different amounts of water. From the water solubility in CO<sub>2</sub> simulated in a previous study, it was calculated that about 0.29 g (3300 ppm) of water will dissolve in 1L of CO<sub>2</sub> under the test conditions (80 bar CO<sub>2</sub> at 50°C).<sup>12</sup> Thus, in the present study, 650, 2000 and 3000 ppm of DI water was added to the autoclave in order to ensure under-saturated conditions.

**TABLE 2**  
**TEST MATRIX FOR EVALUATING WATER CONTENT EFFECT**

CO <sub>2</sub> pressure (bar)	O <sub>2</sub> pressure (bar)	Temperature (°C)	Test period (hour)	Water content (ppm)
80	3.3	50	24	650
80	3.3	50	24	2000
80	3.3	50	24	3000

<sup>(2)</sup> American Petroleum Institute (API), 1220 L St. NW, Washington, DC 20005.

## Effect of SO<sub>2</sub> on the Corrosion of Carbon Steel in the Supercritical CO<sub>2</sub>/O<sub>2</sub> Phase with 650 ppm Water

Table 3 shows the test matrix for corrosion in supercritical CO<sub>2</sub>/O<sub>2</sub>/SO<sub>2</sub> phases with 650 ppm of water. Two types of SO<sub>2</sub> sources were used in the present study: for low concentration of SO<sub>2</sub>, 650 ppm of diluted sulfurous acid (H<sub>2</sub>SO<sub>3</sub>, a solution of SO<sub>2</sub> in water; assay [as SO<sub>2</sub>] 6.0%) was added in the autoclave and 1% of SO<sub>2</sub> gas was added with 650 ppm of DI water for high concentration of SO<sub>2</sub>.

**TABLE 3**  
**TEST MATRIX FOR EVALUATING SO<sub>2</sub> EFFECT**

CO <sub>2</sub> pressure (bar)	O <sub>2</sub> pressure (bar)	SO <sub>2</sub> pressure (bar)	Temperature (°C)	Test period (hour)	Water content (ppm)
80	0	0	50	24	650 (6% H <sub>2</sub> SO <sub>3</sub> )
80	0	0	50	120	650 (6% H <sub>2</sub> SO <sub>3</sub> )
80	3.3	0	50	120	650 (6% H <sub>2</sub> SO <sub>3</sub> )
80	0	0.8	50	24	650
80	3.3	0.8	50	24	650

## RESULTS

### Effect of Water Content on the Corrosion of Carbon Steel in the Supercritical CO<sub>2</sub>/O<sub>2</sub> Phase

Table 4 shows the corrosion rates of carbon steel measured from the weight loss technique under different water contents. There was no evidence of corrosion attack in the supercritical CO<sub>2</sub>/O<sub>2</sub> phase (80 bar CO<sub>2</sub> / 3.3 bar O<sub>2</sub>, 50°C) with 650 and 2000 ppm of water during 24 hours. Normalized weight changes were generally within about 0.1 mg/cm<sup>2</sup> or less, which were considered to be insignificant.

**TABLE 4**  
**CORROSION RATES OF CARBON STEEL WITH DIFFERENT WATER CONTENTS IN SUPERCRITICAL CO<sub>2</sub>/O<sub>2</sub> PHASE**

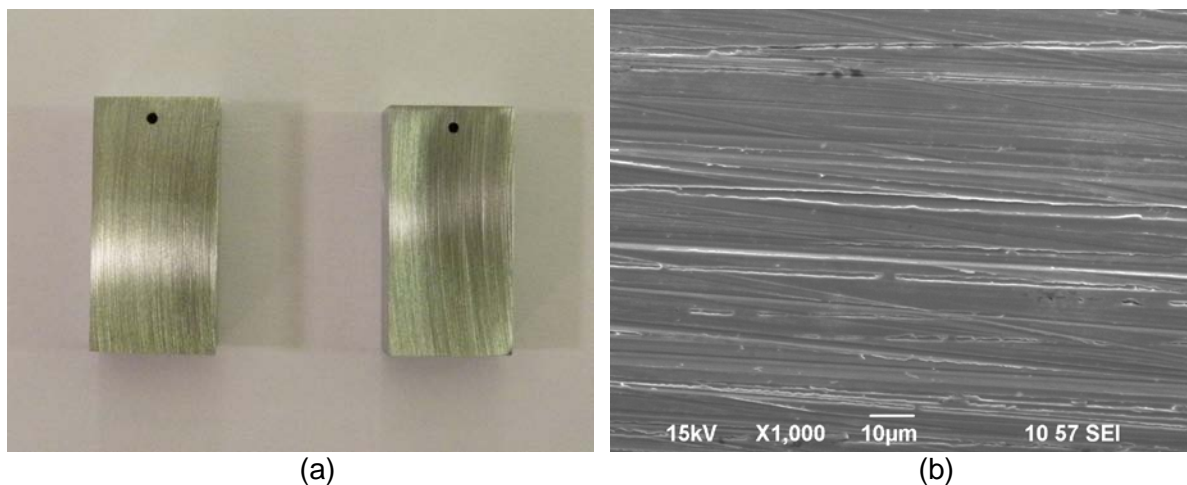
CO <sub>2</sub> pressure (bar)	O <sub>2</sub> pressure (bar)	Temperature (°C)	Test period (hour)	Water content (ppm)	Corrosion rate (mm/y)
80	3.3	50	24	650	< 0.01
80	3.3	50	24	2000	< 0.01
80	3.3	50	24	3000	< 0.01

Figure 1 shows surface appearances of steel samples exposed to the supercritical CO<sub>2</sub>/O<sub>2</sub> phase with 650 ppm of water for 24 hours. No visible signs of corrosion were observed on samples, i.e., the surfaces appeared shiny and void of any type of corrosion products.

However, 3000 ppm of water in the supercritical CO<sub>2</sub>/O<sub>2</sub> phase caused visual signs of corrosion after 24 hours. Figure 2 shows the SEM image and EDS spectra of the surface of the sample after 24 hours in the supercritical CO<sub>2</sub>/O<sub>2</sub> phase with 3000 ppm of water. As shown in Figure 2 (a), very thin corrosion product layers formed on the steel surface.

From EDS analysis, it was shown to mainly consist of iron, carbon and oxygen indicating formation of trace amounts of corrosion products (FeCO<sub>3</sub> or iron oxides) on the steel surface. However, the weight losses of samples were still too small to calculate the corrosion rate (< 0.01 mm/y).

It is noteworthy that the corrosion rate of carbon steel in the water-saturated supercritical CO<sub>2</sub>/O<sub>2</sub> phase (~ 1 mm/y)<sup>6</sup> was much higher than those in the under-saturated conditions. According to a recent study<sup>13</sup>, it is possible that CO<sub>2</sub> dissociates and reacts with other CO<sub>2</sub> or H<sub>2</sub>O molecules to produce corrosion products such as iron carbonate (FeCO<sub>3</sub>), carbonate (CO<sub>3</sub><sup>2-</sup>) or H<sub>2</sub>CO<sub>3</sub> in non-aqueous environments. However, from the present study, it is known that this can happen when the water content exceeds a threshold for onset of corrosion and the threshold water content would be around saturation point under the supercritical CO<sub>2</sub>/O<sub>2</sub> conditions. This also suggests that the current requirement for water content (650 ppm) in the CO<sub>2</sub> pipeline would be sufficient for prevention of corrosion in the supercritical CO<sub>2</sub>/O<sub>2</sub> environments.



**Figure 1: Surface appearances of the sample exposed in the supercritical CO<sub>2</sub>/O<sub>2</sub> phase (80 bar CO<sub>2</sub> / 3.3 bar O<sub>2</sub>, 50°C) with 650 ppm of water for 24 hours: (a) Low magnification photo, (b) SEM image**

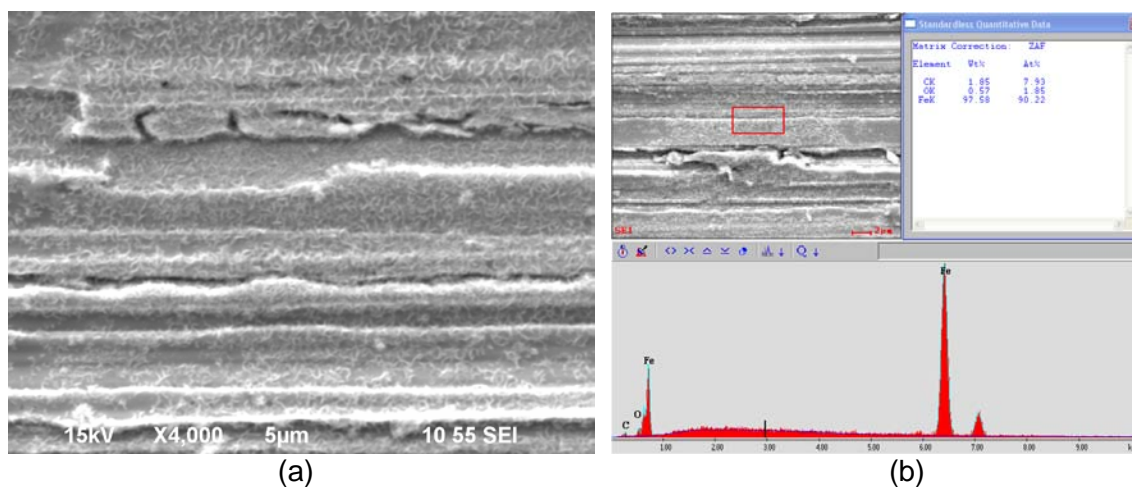


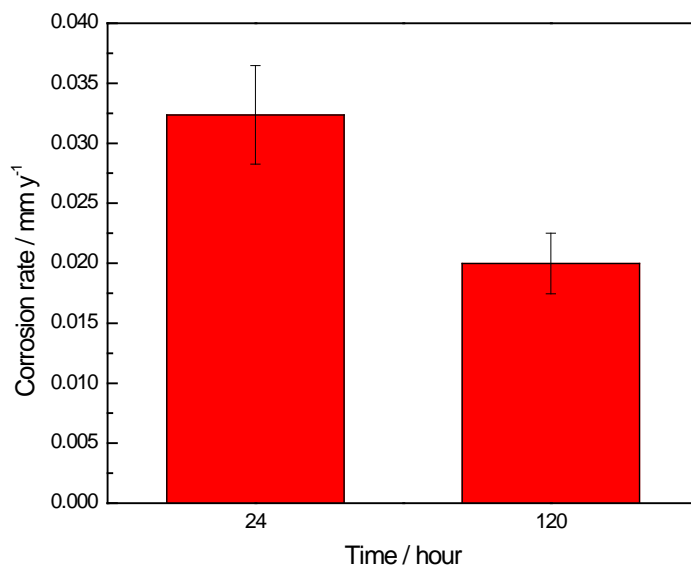
**Figure 2: SEM image (a) and EDS spectra (b) of the surface of sample exposed in the supercritical CO<sub>2</sub>/O<sub>2</sub> phase (80 bar CO<sub>2</sub> / 3.3 bar O<sub>2</sub>, 50°C) with 3000 ppm of water for 24 hours**

## Effect of SO<sub>2</sub> on the Corrosion of Carbon Steel in the Supercritical CO<sub>2</sub>/O<sub>2</sub> Phase with 650 ppm Water

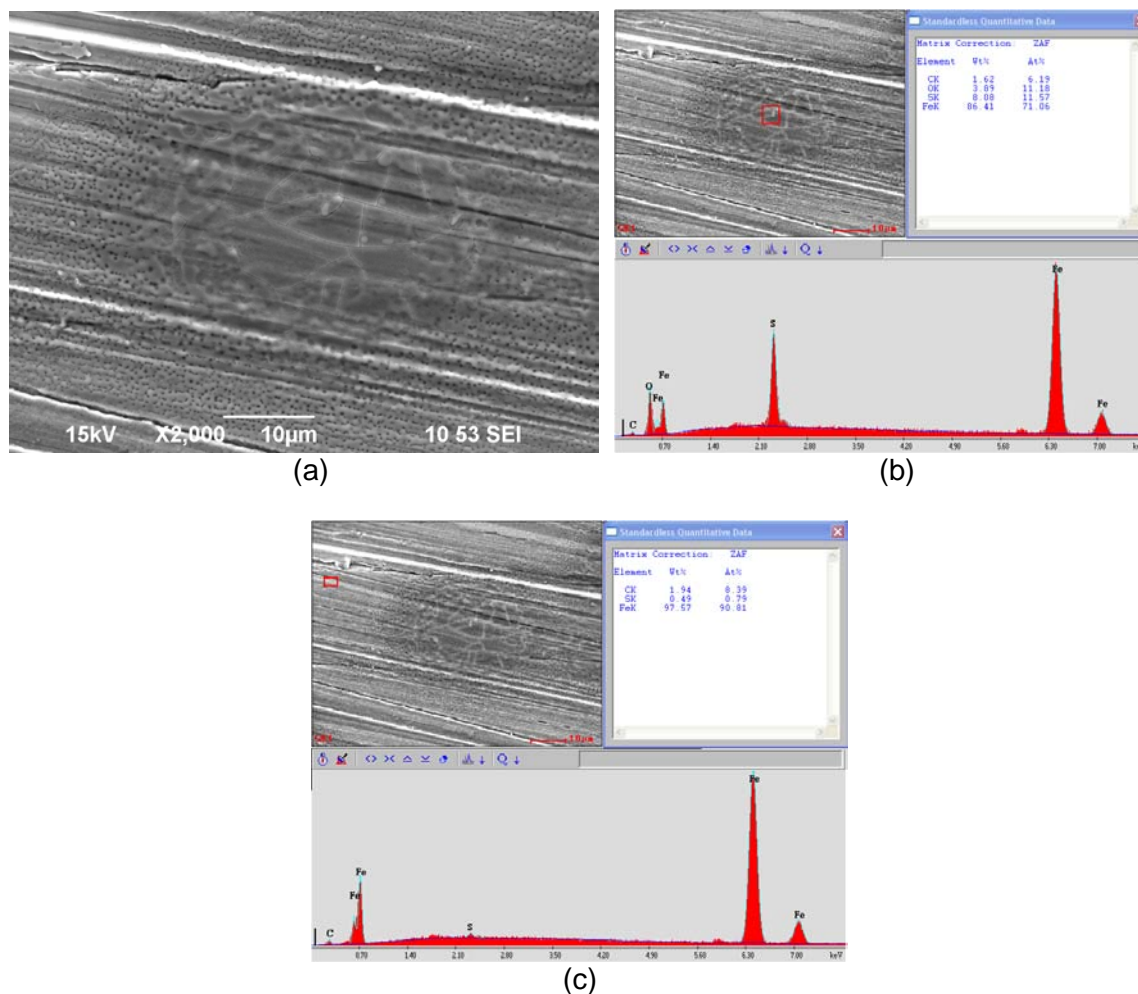
Figure 3 shows the corrosion rates of carbon steel in the supercritical CO<sub>2</sub> phase (80 bar CO<sub>2</sub>, 50°C) with 650 ppm of H<sub>2</sub>SO<sub>3</sub> as a function of test period. As discussed above (Figure 1), there was no evidence of corrosion in the supercritical CO<sub>2</sub>/O<sub>2</sub> phase with 650 ppm of water during 24 hours. However, it can be seen from Figure 3 that trace amount of H<sub>2</sub>SO<sub>3</sub> addition in the supercritical CO<sub>2</sub> phase affected the corrosion of carbon steel although it showed low corrosion rates (0.02 ~ 0.03 mm/y). In addition, the corrosion rate slightly decreased with time because trace amount of H<sub>2</sub>SO<sub>3</sub> solution would react with carbon steel in the beginning of test and deplete with time.

Figure 4 shows the SEM image and EDS spectra of the surface of the sample after 24 hours in the supercritical CO<sub>2</sub> phase (80 bar CO<sub>2</sub>, 50°C) with 650 ppm of H<sub>2</sub>SO<sub>3</sub>. As shown in Figure 4 (a), thin corrosion product layers locally formed on the steel surface with a blister shape. From EDS analysis, it was determined to mainly consist of iron, sulfur and oxygen indicating formation of iron sulfate (FeSO<sub>4</sub>) or iron sulfite (FeSO<sub>3</sub>) on the steel surface (Figure 4 (b)), however negligible amounts of sulfur and oxygen were detected on the steel surface where no corrosion products were present (Figure 4 (c)).

This indicates that the addition of H<sub>2</sub>SO<sub>3</sub> results in the formation of these thin corrosion products under the supercritical CO<sub>2</sub> condition and it can increase the corrosion rate of the steel even though it is completely dissolved in the supercritical CO<sub>2</sub> phase (under-saturation). However, no localized corrosion was observed under the corrosion products after cleaning the surface with Clarke solution because of the low average corrosion rate.



**Figure 3: Effects of H<sub>2</sub>SO<sub>3</sub> and exposure time on the corrosion rates of carbon steel in the supercritical CO<sub>2</sub> phase (80 bar CO<sub>2</sub>, 50°C)**



**Figure 4: SEM image and EDS spectra of the corroded surface of sample exposed to the supercritical CO<sub>2</sub> phase (80 bar CO<sub>2</sub>, 50°C) with 650 ppm of H<sub>2</sub>SO<sub>3</sub> for 24 hours: (a) SEM image, (b) EDS analysis of the corrosion product, (c) EDS analysis of the surface without corrosion product.**

Figure 5 shows the SEM image and EDS spectra of the surface of the sample after 120 hours in the supercritical CO<sub>2</sub> phase with 650 ppm of H<sub>2</sub>SO<sub>3</sub>. In this case, and compared with Figure 4, the sulfur-bearing thin corrosion product layers covered the entire steel surface.

SO<sub>2</sub> has been recognized as the main corrosive gaseous air pollutant in the atmosphere and it enhances the corrosion rates of metals exposed in the atmosphere.<sup>14-16</sup> Currently, the established model for the atmospheric corrosion of steel in the presence of SO<sub>2</sub> is through “sulfate nests”.<sup>17</sup> Sulfate nests are blisters, formed spatially heterogeneous on the surface, and containing high concentrations of corrosion products. The formation, distribution and size of these sulfate nests are mainly dependent on the SO<sub>2</sub> concentration of the environment and the time of exposure.<sup>18</sup>

The morphologies of the sulfur-bearing corrosion products shown in Figures 4 and 5 are somewhat similar to that of sulfate nests from the atmospheric corrosion. Thus, it can be assumed that the role of SO<sub>2</sub> or H<sub>2</sub>SO<sub>3</sub> on the corrosion under supercritical CO<sub>2</sub> phase would be similar to that in atmospheric corrosion since it happens under a thin water layer on the hydrophilic steel surface.

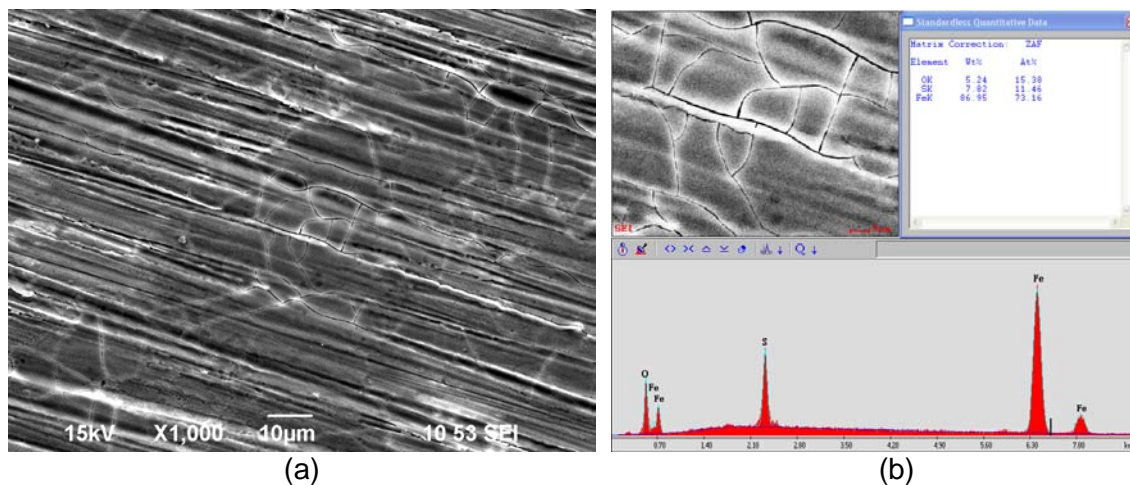


**Figure 5: SEM image (a) and EDS spectra (b) of the corroded surface of sample exposed to supercritical CO<sub>2</sub> with 650 ppm of H<sub>2</sub>SO<sub>3</sub> for 120 hours**

Figure 6 shows the corrosion rate of carbon steel in the supercritical CO<sub>2</sub>/O<sub>2</sub> phase with 650 ppm of H<sub>2</sub>SO<sub>3</sub> compared with that in the supercritical CO<sub>2</sub> phase. Although the addition of O<sub>2</sub> in the system slightly increases the corrosion rate of carbon steel, it showed low corrosion rates (< 0.03 mm/y).

Figures 7 and 8 show the SEM images and EDS spectra of the surfaces of the sample after 120 hours in the supercritical CO<sub>2</sub>/O<sub>2</sub> phase with 650 ppm of H<sub>2</sub>SO<sub>3</sub>. As shown in Figure 7, elongated-globular shaped corrosion products formed locally on the steel surface and blisters were formed under these corrosion products.

From EDS analysis, these were found to mainly consist of iron, carbon, sulfur and oxygen (Figure 8 (a)), but lower sulfur content was detected than in the supercritical CO<sub>2</sub> phase. This indicates that the sulfur-bearing corrosion products exist underneath the elongated-globular shaped product, which may be an iron oxide due to the addition of O<sub>2</sub>.

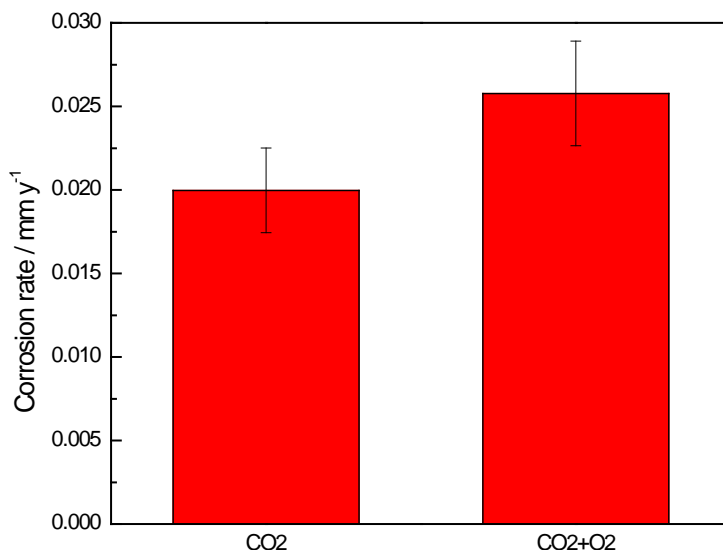


**Figure 6: Effects of oxygen on the corrosion rates of carbon steel in supercritical CO<sub>2</sub> phase with 650 ppm H<sub>2</sub>SO<sub>3</sub>**

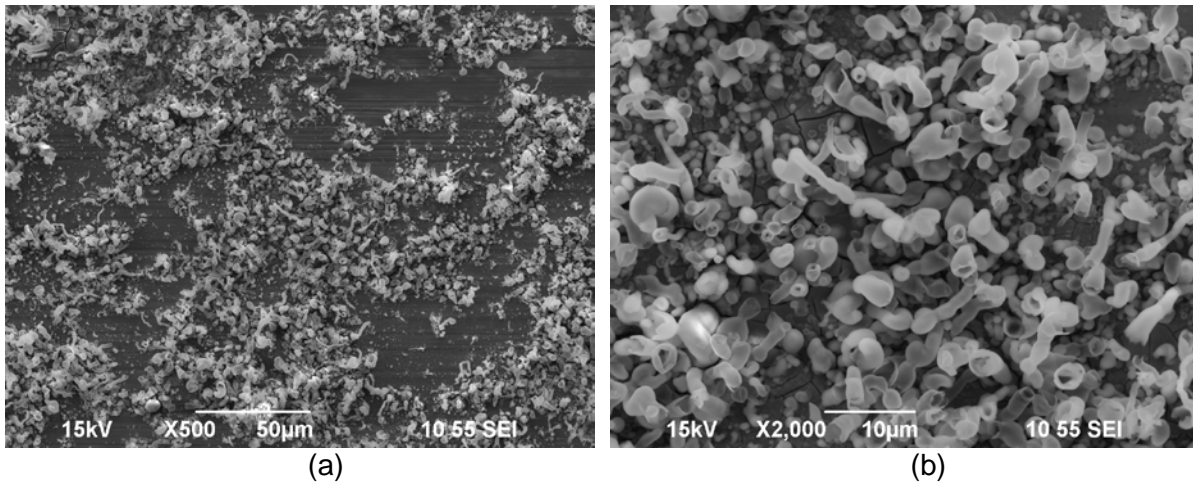


**Figure 7: SEM images of the corroded surface of sample exposed to supercritical CO<sub>2</sub>/O<sub>2</sub> with 650 ppm of H<sub>2</sub>SO<sub>3</sub> for 120 hours: (a) low magnification, (b) high magnification**

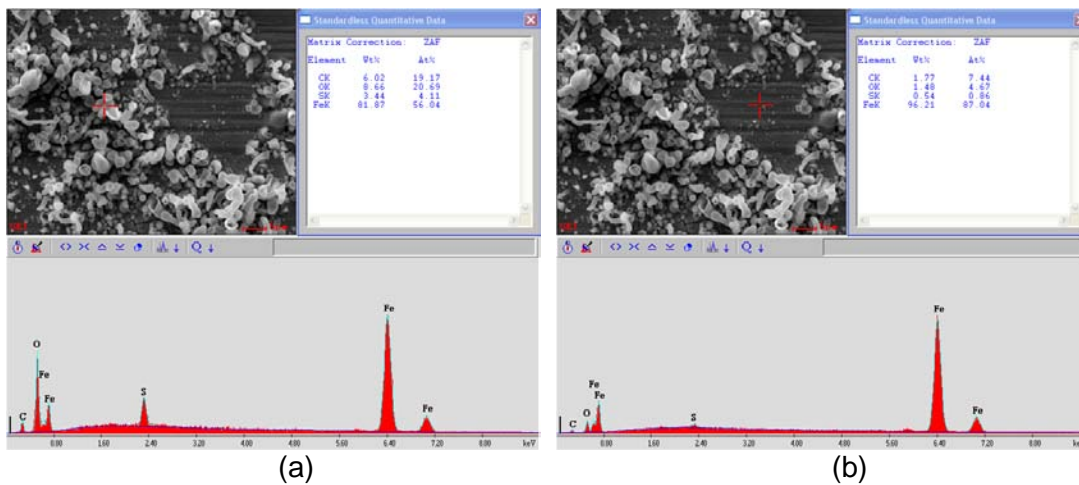


**Figure 8: EDS spectra of the corroded surface of sample exposed to supercritical CO<sub>2</sub>/O<sub>2</sub> with 650 ppm of H<sub>2</sub>SO<sub>3</sub> for 120 hours: (a) corrosion product area, (b) uncovered substrate area**

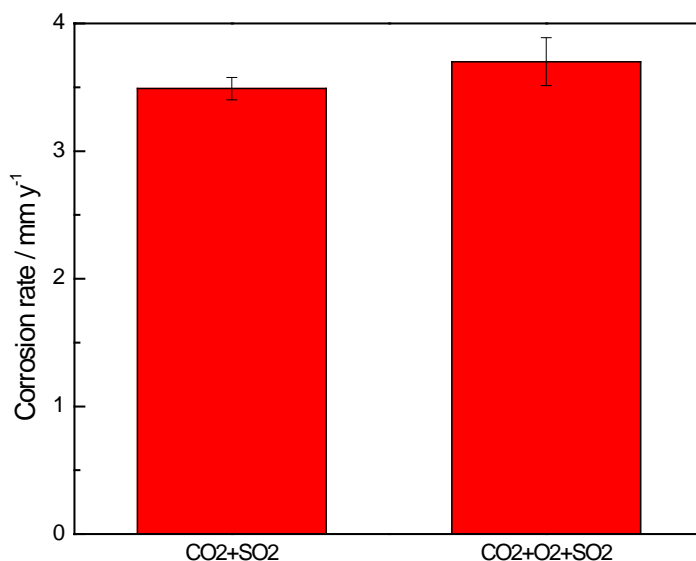
Figure 9 represents the effect of O<sub>2</sub> (4% in gas phase, 3.3 bar) and SO<sub>2</sub> (1% in gas phase, 0.8 bar) additions on the corrosion rates of carbon steel in the supercritical CO<sub>2</sub> phase (80 bar CO<sub>2</sub>, 50°C) with 650 ppm of water. As shown in Figure 9, the addition of 1% SO<sub>2</sub> in the gas phase dramatically increased the corrosion rates of carbon steel to 3.5 mm/y and it slightly increases to 3.7 mm/y with addition of both O<sub>2</sub> and SO<sub>2</sub>. This indicates that high concentration of SO<sub>2</sub> can accelerate the corrosion reaction in the supercritical CO<sub>2</sub> phase with a trace amount of water.

Figure 10 compares the corrosion rates of carbon steel in the supercritical CO<sub>2</sub>/O<sub>2</sub>/SO<sub>2</sub> mixtures (80 bar CO<sub>2</sub>, 3.3 bar O<sub>2</sub>, 0.8 bar SO<sub>2</sub>, 50°C) with different amounts of water. The corrosion rates measured in saturated conditions (3310 ppm water) were taken from our previous results.<sup>6</sup>

It showed no corrosion in the supercritical CO<sub>2</sub> and the supercritical CO<sub>2</sub>/O<sub>2</sub> phases with 650 ppm water, while it presented relatively high corrosion rates (0.4 and 1 mm/y) in the same phases with 3310 ppm water (saturated condition). This again confirms that corrosion can be prevented by decreasing water content in supercritical CO<sub>2</sub>/O<sub>2</sub> phases.

However, catastrophically high corrosion rates were measured under the supercritical  $\text{CO}_2/\text{SO}_2$  and the supercritical  $\text{CO}_2/\text{O}_2/\text{SO}_2$  phases in both saturated and under-saturated conditions; this is ascribed to the addition of a high concentration of  $\text{SO}_2$ , which increases the corrosion rate of the steel in both conditions regardless of water content. This can be attributed to the synergism between water and  $\text{SO}_2$  described above.

Figures 11 and 12 show the SEM images of the surface of the sample after 24 hours in the supercritical  $\text{CO}_2/\text{SO}_2$  and the supercritical  $\text{CO}_2/\text{O}_2/\text{SO}_2$  mixtures with 650 ppm of water, respectively. As shown in Figure 11, the surface was covered by corrosion products which show dendritic growth under the supercritical  $\text{CO}_2/\text{SO}_2$  condition. However, the surface showed cracks and secondary corrosion products when the sample was exposed to the supercritical  $\text{CO}_2$  phase with  $\text{O}_2$  and  $\text{SO}_2$ .



**Figure 9: Effects of oxygen (3.3 bar) and sulfur dioxide (0.8 bar) on the corrosion rates of carbon steel in the supercritical  $\text{CO}_2$  phase (80 bar  $\text{CO}_2$ , 50°C) with 650 ppm water**

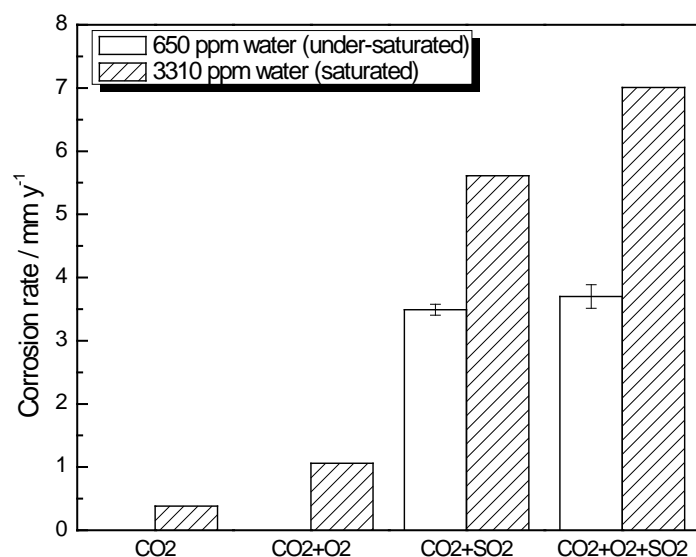


**Figure 10: Comparison of the corrosion rates of carbon steel in the supercritical  $\text{CO}_2/\text{O}_2/\text{SO}_2$  mixtures (80 bar  $\text{CO}_2$ , 3.3 bar  $\text{O}_2$ , 0.8 bar  $\text{SO}_2$ , 50°C) with different amounts of water**

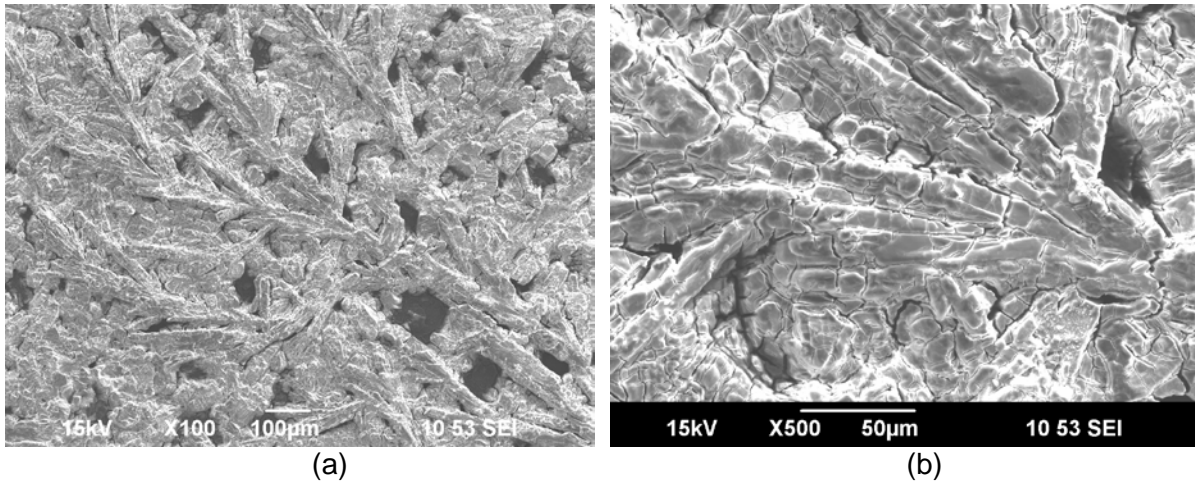


**Figure 11: SEM images of the corroded surface of sample exposed in the supercritical  $\text{CO}_2/\text{SO}_2$  phase (80 bar  $\text{CO}_2$ , 0.8 bar  $\text{SO}_2$ ,  $50^\circ\text{C}$ ) with 650 ppm of water for 24 hours: (a) low magnification, (b) high magnification**

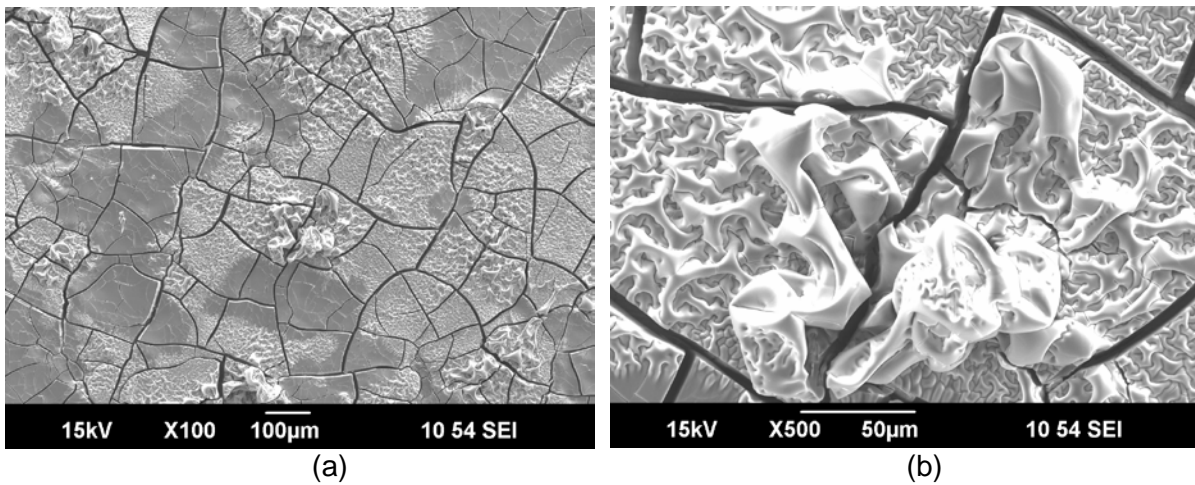


**Figure 12: SEM images of the corroded surface of sample exposed in the supercritical  $\text{CO}_2/\text{O}_2/\text{SO}_2$  phase (80 bar  $\text{CO}_2$ , 3.3 bar  $\text{O}_2$ , 0.8 bar  $\text{SO}_2$ ,  $50^\circ\text{C}$ ) with 650 ppm of water for 24 hours: (a) low magnification, (b) high magnification**

Figures 13 and 14 show the EDS spectra of the sample surfaces after 24 hours in the supercritical  $\text{CO}_2/\text{SO}_2$  and the supercritical  $\text{CO}_2/\text{O}_2/\text{SO}_2$  mixtures with 650 ppm of water, respectively. Even though the morphologies of the corrosion products are different between those two cases, the corrosion products consisted of iron, sulfur and oxygen for both conditions.

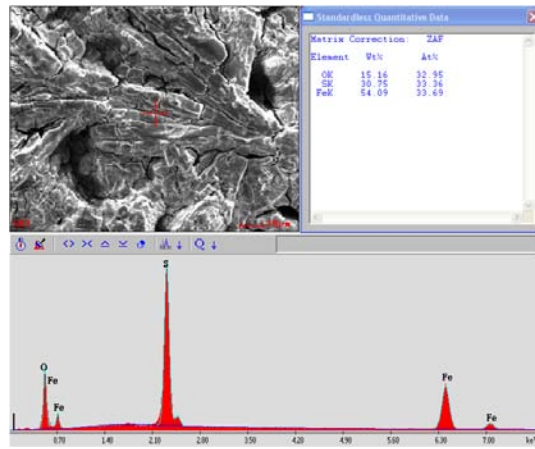


**Figure 13: EDS spectrum of the corroded surface of sample exposed in the supercritical CO<sub>2</sub>/SO<sub>2</sub> phase with 650 ppm of water for 24 hours**

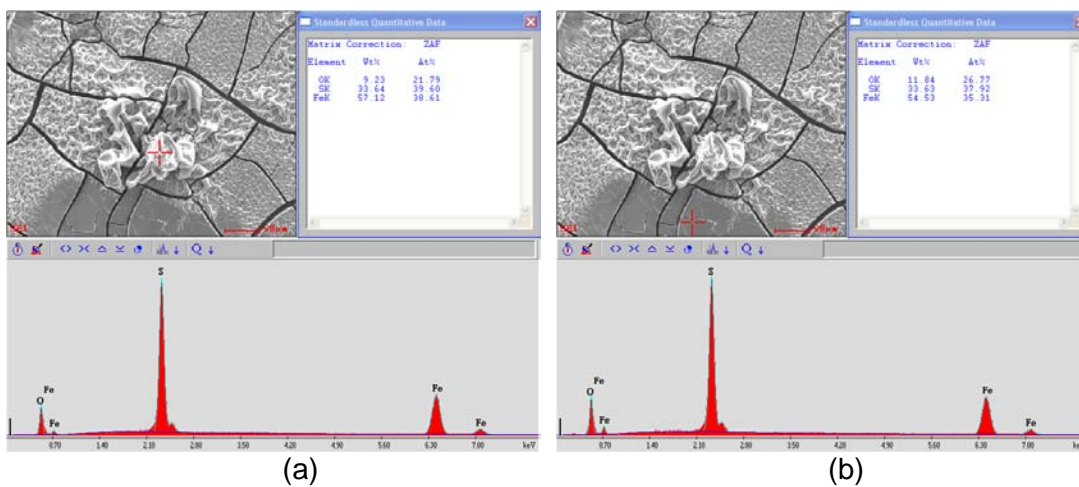


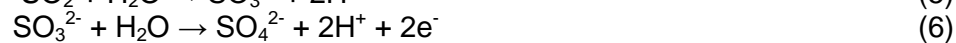
**Figure 14: EDS spectra of the corroded surface of sample exposed in the supercritical CO<sub>2</sub>/O<sub>2</sub>/SO<sub>2</sub> mixture with 650 ppm of water for 24 hours: (a) primary corrosion product area, (b) secondary corrosion product area**

XRD analysis shown in Figure 15 indicates that the corrosion products mainly consisted of FeSO<sub>3</sub> hydrate and FeSO<sub>4</sub> hydrate when carbon steel was exposed to the supercritical CO<sub>2</sub>/SO<sub>2</sub> phase with 650 ppm water. However, no significant peaks were detected from the sample exposed in the supercritical CO<sub>2</sub>/O<sub>2</sub>/SO<sub>2</sub> mixture with 650 ppm water. This suggests that the corrosion products formed on the surface could be an amorphous structure which cannot be detected by XRD.

The formation of FeSO<sub>3</sub>·xH<sub>2</sub>O and FeSO<sub>4</sub>·xH<sub>2</sub>O has been observed as corrosion products of Fe at low relative humidity and high concentration of SO<sub>2</sub> in atmospheric corrosion conditions.<sup>14,19</sup> Thus, as mentioned above, the role of SO<sub>2</sub> on the corrosion under supercritical CO<sub>2</sub> phase would be similar to that in atmospheric corrosion. The formation of FeSO<sub>3</sub> by adding SO<sub>2</sub> in the gas phase can be described as follows:<sup>20</sup>



The formation of FeSO<sub>4</sub> by adding SO<sub>2</sub> in the gas phase can similarly be described:<sup>21</sup>



This indicates that the addition of SO<sub>2</sub> in the gas phase can synergistically lower the pH of the electrolyte and increase the corrosion rates of the steel even though water is dissolved in the CO<sub>2</sub> phase.

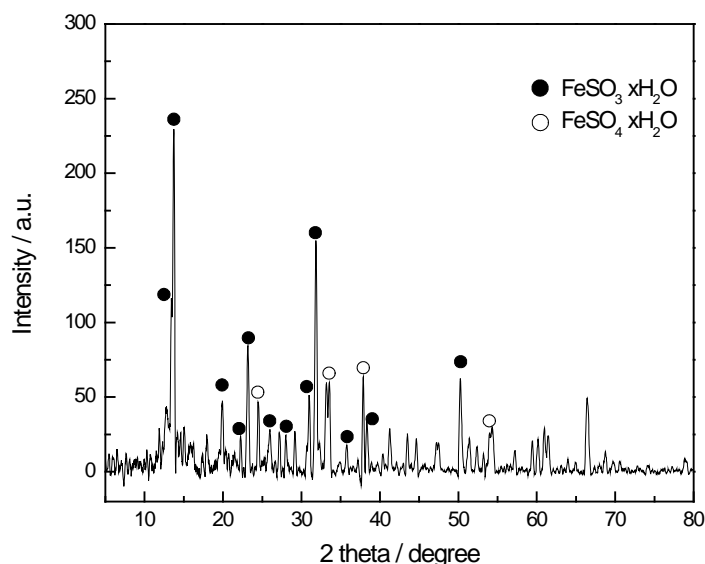


**Figure 15: XRD result of the corroded surface of sample exposed in the supercritical CO<sub>2</sub>/SO<sub>2</sub> phase with 650 ppm of water for 24 hours**

Table 5 reports a summary of measured corrosion rates under different conditions with 650 ppm of water.

**TABLE 5  
CORROSION RATES OF CARBON STEEL IN SUPERCRITICAL CO<sub>2</sub>/O<sub>2</sub>/SO<sub>2</sub> MIXTURES WITH 650 PPM WATER**

CO <sub>2</sub> pressure (bar)	O <sub>2</sub> pressure (bar)	SO <sub>2</sub> pressure (bar)	Temperature (°C)	Test period (hour)	Water content (ppm)	Corrosion rate (mm/y)
80	0	0	50	24	650 (6% H <sub>2</sub> SO <sub>3</sub> )	0.032
80	0	0	50	120	650 (6% H <sub>2</sub> SO <sub>3</sub> )	0.019
80	3.3	0	50	120	650 (6% H <sub>2</sub> SO <sub>3</sub> )	0.025
80	0	0.8	50	24	650	3.48
80	3.3	0.8	50	24	650	3.70

## CONCLUSIONS

The corrosion properties of carbon steel in supercritical CO<sub>2</sub>/O<sub>2</sub>/SO<sub>2</sub> mixtures with different amounts of water (under-saturated) were investigated by weight loss measurements and surface analysis techniques. The following conclusions are drawn:

- There was no significant corrosion attack in the supercritical CO<sub>2</sub>/O<sub>2</sub> phase with 650, 2000 and 3000 ppm of water.
- Supercritical CO<sub>2</sub> and supercritical CO<sub>2</sub>/O<sub>2</sub> phases with 650 ppm of H<sub>2</sub>SO<sub>3</sub> caused visually obvious signs of corrosion with low corrosion rates (0.02 ~ 0.03 mm/y).
- Based on the assay of H<sub>2</sub>SO<sub>3</sub> (6% of SO<sub>2</sub> in water), trace amount of SO<sub>2</sub> in water can affect the corrosion of carbon steel in the supercritical CO<sub>2</sub> phase.
- The addition of 1% SO<sub>2</sub> in the gas phase dramatically increased the corrosion rate of carbon steel to 3.5 mm/y with 650 ppm of water. This then slightly increased to 3.7 mm/y with addition of both O<sub>2</sub> and SO<sub>2</sub>.
- Significant corrosion was observed with 1% SO<sub>2</sub> under the current guideline for water content in CO<sub>2</sub> pipelines (650 ppm).

## ACKNOWLEDGEMENTS

The authors would like to acknowledge the financial support from Ohio Coal Development Office (OCDO) for the Institute for Corrosion and Multiphase Technology at Ohio University. And the authors are grateful to Dr. D. Young (Ohio University) for scientific discussion.

## REFERENCES

1. IPCC Special Report, “*Carbon Dioxide Capture and Storage: Technical Summary*” (2005), p. 181.
2. M. Seiersten, K.O. Kongshaug, “Materials Selection for Capture, Compression, Transport and Injection of CO<sub>2</sub>”, *Carbon Dioxide Capture for Storage in Deep Geologic Formations*, Volume 2, (Elsevier, 2005), p. 937.
3. G. Heggum, T. Weydahl, M. Molnvik, A. Austegaard, “CO<sub>2</sub> Condition and Transportation”, *Carbon Dioxide Capture for Storage in Deep Geologic Formations*, Volume 2, (Elsevier, 2005), p. 925.
4. D.P. Connell, “Carbon Dioxide Capture Options for Large Point Sources in the Midwestern United States: An Assessment of Candidate Technologies,” Final Report, CONSOL Energy Inc., p. 7 (2005).
5. K.D. Kaufmann, “Impurity Types, Concentration Influence Hydraulic Design,” *Oil & Gas Journal* 108, 14 (2010): p. 60.
6. Y.S. Choi, S. Netic, “Effect of Impurities on the Corrosion Behavior of Carbon Steel in Supercritical CO<sub>2</sub>-Water Environments,” CORROSION/2010, paper no. 10196 (Houston, TX: NACE, 2010).
7. B.P. McGrail, H.T. Schaefer, V.A. Glezakou, L.X. Dang, A.T. Owen, “Water Reactivity in the Liquid and Supercritical CO<sub>2</sub> Phase: Has Half the Story been Neglected?” *Energy Procedia* 1 (2009): p. 3415.
8. R. Thodla, F. Ayello, N. Sridhar, “Materials Performance in Supercritical CO<sub>2</sub> Environments”, CORROSION/2009, paper no. 09255, (Houston, TX: NACE, 2009).
9. B.M. Sass, H. Farzan, R. Prabhakar, J. Gerst, J. Sminchak, M. Bhargava, B. Nestleroth, J. Figueroa, “Consideration of Treating Impurities in Oxy-Combustion Flue Gas Prior to Sequestration,” *Energy Procedia*, 1 (2009): p. 535.
10. ASTM Standard G1-03, “Standard Practice for Preparing, Cleaning, and Evaluating Corrosion Test Specimens,” in Annual Book of ASTM Standards, vol. 03. 02 (West Conshohocken, PA: ASTM International, 2003)

11. ASTM Standard G31, "Standard Practice for Laboratory Immersion Corrosion Testing of Metals," in Annual Book of ASTM Standards, vol. 03. 02 (West Conshohocken, PA: ASTM International, 1994)
12. Y.S. Choi, S. Nescic, "Corrosion Behavior of Carbon Steel in Supercritical CO<sub>2</sub>-Water Environments," CORROSION/2009, paper no. 09256 (Houston, TX: NACE, 2009).
13. V.A. Glezakou, L.X. Dang, B.P. McGrail, "Spontaneous Activation of CO<sub>2</sub> and Possible Corrosion Pathways on the Low-Index Iron Surface Fe(100)," *J. Phys. Chem. C* 113, 9 (2009): p. 3691.
14. T.E. Graedel, R.P. Frankenthal, "Corrosion Mechanisms for Iron and Low Alloy Steels Exposed to the Atmosphere," *J. Electrochem. Soc.* 137, 8 (1990): p. 2385.
15. W. McLeod, R.R. Rogers, "Sulfurous Acid Corrosion of Low Carbon Steel at Ordinary Temperatures- 1. Its Nature," *Corrosion* 22, 5 (1966): p. 143.
16. C. Leygraf, T. Graedel, *Atmospheric Corrosion* (New York, John Willey & Sons, 2000).
17. J. Weissenrieder, C. Kleber, M. Schreiner, C. Leygraf, "In Situ Studies of Sulfate Nest Formation on Iron," *J. Electrochem. Soc.* 151, 9 (2004): p. B497.
18. S. Oesch, "Environmental Effects on Materials; Effect of SO<sub>2</sub> on the Corrosion of Unalloyed Steel and Weathering Steel – an Attempt to Simulate Atmospheric Corrosion," *Materials and Corrosion* 47, 9 (1996): p. 505.
19. L.-G. Johansson, O. Lindqvist, "The Crystal Structure of Iron(II) Sulfite Trihydrate,  $\alpha$ -FeSO<sub>3</sub>·3H<sub>2</sub>O," *Acta Cryst.* B35, 5 (1979): p. 1017.
20. J.F. Marco, J. Davalos, J.R. Gancendo, M. Gracia, "Mössbauer Study of the Corrosion Behavior of Pure Iron and Weathering Steel under a Wet-Dry Cycle," *Hyperfine Interactions* 46, 1-4 (1989): p. 453.
21. R. Nishimura, D. Shiraishi, Y. Maeda, "Hydrogen Permeation and Corrosion Behavior of High Strength Steel MCM 430 in Cyclic Wet–Dry SO<sub>2</sub> Environment," *Corrosion Science* 46, 1 (2004): p. 225.